

Green Chemistry

Cutting-edge research for a greener sustainable future

Accepted Manuscript

View Article Online
View Journal

This article can be cited before page numbers have been issued, to do this please use: W. Wang, J. Wang, Y. Pi, C. Li and R. Tan, *Green Chem.*, 2020, DOI: 10.1039/D0GC00949K.



This is an Accepted Manuscript, which has been through the Royal Society of Chemistry peer review process and has been accepted for publication.

Accepted Manuscripts are published online shortly after acceptance, before technical editing, formatting and proof reading. Using this free service, authors can make their results available to the community, in citable form, before we publish the edited article. We will replace this Accepted Manuscript with the edited and formatted Advance Article as soon as it is available.

You can find more information about Accepted Manuscripts in the [Information for Authors](#).

Please note that technical editing may introduce minor changes to the text and/or graphics, which may alter content. The journal's standard [Terms & Conditions](#) and the [Ethical guidelines](#) still apply. In no event shall the Royal Society of Chemistry be held responsible for any errors or omissions in this Accepted Manuscript or any consequences arising from the use of any information it contains.

Cite this: DOI: 10.1039/c0xx00000x

www.rsc.org/xxxxxx

ARTICLE TYPE

Iron(II)-folded single-chain nanoparticle: a metalloenzyme mimicking sustainable catalyst for highly enantioselective sulfa-Michael addition in water

Weiyang Wang, Jiajun Wang, Shiye Li, Chaoping Li, Rong Tan* and Donghong Yin

Received (in XXX, XXX) Xth XXXXXXXXX 200X, Accepted Xth XXXXXXXXX 200X

DOI: 10.1039/b000000x

Metalloenzyme is a source of inspiration for chemists who attempt to create versatile synthetic catalysts for aqueous catalysis. Herein, we impart metalloenzyme-like characteristics to chiral Fe^{II}-oxazoline complex by incorporating Fe(II) ion into chiral oxazoline-containing discrete self-folded polymer, to realize the highly enantioselective sulfa-Michael addition (SMA) in water. Intrachain Fe^{II}-oxazoline complexation together with hydrophobic interaction triggers the self-folding of oxazoline-containing single polymeric chain in water. The formed Fe^{II}-folded single-chain polymeric nanoparticles (SCPNs) significantly accelerate the aqueous asymmetric SMA reaction *via* self-folded hydrophobic compartment around the catalytic sites, reminiscent of metalloenzymatic catalysis. In addition, they can be facilely recovered for reuse by simple thermo-controlled separation due to thermo-responsive properties. Such metallo-folded SCPNs combine the benefits of transition metal- and bio-catalyst, and avoid the tedious procedures for separation, which is a benefit for energy-saving and industrial applications.

Introduction

Asymmetric sulfa-Michael addition (SMA) is of great importance in asymmetric synthesis, since it provides direct access to enantioenriched sulfides that are versatile precursors for the synthesis of bioactive compounds.¹ Several catalytic systems, including cinchona alkaloid derivatives,² heterobimetallic complexes,³ and organocatalysts,^{1c,4} have been developed specifically for this transformation. In spite of impressive progress, most of them suffer from certain limitations, such as low reaction temperatures (-10 to -60 °C),^{1d,2a,4a,4e} high catalyst loading (10-20 mol%),^{1b,4a,4c,4e} use of harsh additives (strong acid),^{4b} and the requirement of halogenated or aromatic solvents (dichloromethane or toluene),²⁻⁴ which restrict the large-scale application in industry (Scheme 1). Recently, iron-based chiral complex have emerged to catalyze the asymmetric conjugate additions at room temperature without the use of any additives.⁵ Nonetheless, industrial practice is still limited by the use of halogenated solvents (dichloroethane) which often results in

environmental problems. Water undoubtedly is an ideal solvent for the asymmetric SMA from economical and environmental points of view. More importantly, water was reported to stabilize the transition state of SMA *via* weak hydrogen bonding, which enhanced the enantioselectivity.^{2c} Yet, few attempt has been made to efficiently perform the asymmetric SMA in water, because of the poor water-solubility of substrates and/or catalysts, as well as the competitive complexation of water to metal center.

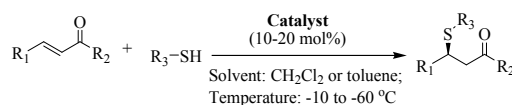
In nature, metalloenzymes regulate a broad variety of biochemical reactions efficiently in aqueous bioenvironment.⁶ The high catalytic efficiency is a result of the guided three-dimensional folding of a single polypeptide chain, which gives a compartmentalized structure with hydrophobic cores surrounded by hydrophilic shells.⁷ Amino acid residues often act as ligands to coordinate with metal ions upon the single-chain folding, forming the inner compartment that acts as an 'active site'. The intriguing metalloenzyme catalysis inspired us to mimic these natural catalytic compartments where the catalytically active cores are isolated from the surrounding aqueous environment, so as to realize efficient SMA reactions in water. Incorporating metal ions into discrete self-folded polymer chains through intramolecular chelation offers a facile way to prepare synthetic mimics of metalloenzymes.⁸ Apart from operating as triggers for the chain-collapse, the formed metal complex embedding into the compartmentalized SCPN structure allows them to function as isolated catalytic center. The unique structural features are highly reminiscent of those contributing to the effectiveness of metalloenzymes. These fascinating features encouraged us to reason that coordination-driven self-folding strategy could be used to construct Fe^{II}-folded SCPNs and allowed for highly enantioselective SMA reaction in water.

* National & Local Joint Engineering Laboratory for New Petrochemical Materials and Fine Utilization of Resources; Key Laboratory of Chemical Biology and Traditional Chinese Medicine Research (Ministry of Education); Key Laboratory of the Assembly and Application of Organic Functional Molecules of Hunan Province, Hunan Normal University, Changsha 410081 (P. R. China).

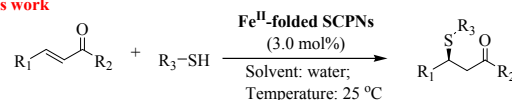
E-mail: yiyangtanrong@126.com

Electronic Supplementary Information (ESI) available: Identity of copolymer precursors of PN_xO_y, synthesis of α , β -unsaturated ketones, as well as detailed NMR spectra and HPLC analysis for chiral β -thioketones. See DOI: 10.1039/x0xx00000x

a) Previous work



b) This work

**Scheme 1** Asymmetric catalysis of SMA to α , β -unsaturated ketones

Since oxazolines are hydrophobic ligands suitable for the coordination of iron ion,⁹ we appended multiple chiral oxazoline ligands as structure-forming elements on an amphiphilic random copolymer. It is expected that the chiral oxazoline ligands would undergo intrachain chelation with iron ion, triggering self-folding of the copolymer into water-soluble SCPNs. Hydrophobic compartment should be thus created around the catalytic iron centers, serving as a catalytic cavity for efficient asymmetric SMA in water. Water is strongly retarded into the hydrophobic compartment,¹⁰ minimizing the undesired competitive complexation to Fe(II) center. Unfortunately, the hydrophilic shell may make the SCPNs difficult to be recovered from water. If the shell is thermo-sensitive, being able to undergo reversible hydrophilic/hydrophobic switch at its cloud-point, facile recovery of the SCPNs can be realized. Herein, the oxazoline-containing monomer was copolymerized with thermo-sensitive *N*-isopropylacrylamide (NIPAAm)¹¹ via reversible addition fragmentation chain transfer (RAFT) polymerization.¹² Treatment of the copolymers with FeCl₂ solution under highly diluted conditions gave the Fe^{II}-folded SCPNs with a hydrophobic Fe^{II}-oxazoline core surrounded by a thermosensitive NIPAAm shell. At the reaction temperature (25 °C), the SCPNs are water-soluble, and induced highly enantioselective SMA in water via the self-folded hydrophobic compartment around the catalytic sites, reminiscent of metalloenzymatic catalysis. Only 3.0 mol% of the Fe^{II}-folded SCPNs was sufficient to give almost quantitative yield (90-96%) of a wide range of chiral β -thioketones with high enantioselectivity (90-99%) in water without the use of any additives. After the reaction, the catalysts turned hydrophobic upon heating, allowing for the facile recovery of catalysts for steady reuse. More interestingly, the activity switching was repeatable even after seven heating/cooling cycles.

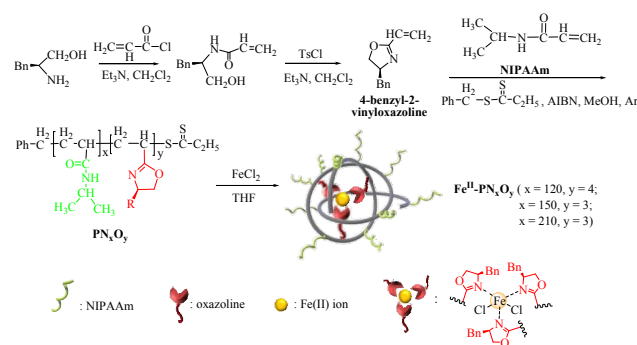
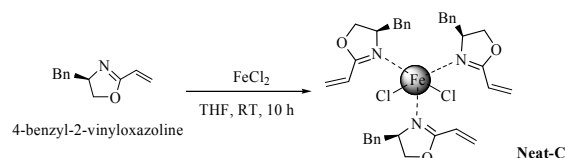
Results and Discussion

Preparation and Characterization of Catalysts

Metalloenzymes achieved efficient catalysis in aqueous bioenvironment via a hydrophobic compartment that isolates the active metal center.^{6,7} It is a source of inspiration for chemists who sought to perform organic reactions in water. Folding of a single random copolymer chain into compartmentalized SCPNs is a simple and feasible approach for constructing the enzyme-like compartment.^{7c,8} In particular, if active metal sites are isolated in their hydrophobic compartments, it endows the SCPNs with enzyme-mimetic activity and selectivity in aqueous catalysis.⁸ Therefore, we decided to shield Fe(II) ion in a water-soluble SCPN compartment to fabricate a metalloenzyme-mimetic catalyst for highly enantioselective SMA in water. Intrachain

metal-coordination strategy has been employed to driven the single-chain folding. Given that chiral oxazoline is a suitable ligand for Fe(II) ion,⁹ we thus prepared the random copolymers of poly(NIPAAm-*co*-oxazoline) (denoted as PN_xO_y) with NIPAAm and oxazoline pendants random distributed along the polymer backbone. The molar ration of NIPAAm/oxazoline per chain was adjusted elaborately to promote the self-folding of PN_xO_y. We envisioned that the hydrophobic oxazoline pendants would serve as handles for concurrent binding/folding via intrachain Fe(II) complexation. And the thermo-responsive NIPAAm side chains may impart inverse temperature-dependent water-solubility to the resulted SCPNs. The obtained Fe^{II}-PN_xO_y should not only achieve highly enantioselective SMA in water as a result of the “biomimetic catalysis”, but also be facilely recovered by thermo-controlled separation. The synthesis of Fe^{II}-PN_xO_y was illustrated in Scheme 2.

Since reversible addition-fragmentation chain transfer (RAFT) polymerization provides fine control over the molar mass,¹² the parent random copolymers of PN_xO_y were synthesized via RAFT technology by using *N*, *N*-azobis(isobutyronitrile) (AIBN) and benzyl dithiopropionate as the radical initiator and chain transfer agent, respectively. Polymerization degrees of the NIPAAm and oxazoline monomers were verified by ¹H NMR in CDCl₃ by comparing the signals attributable to individual blocks (NIPAAm at *ca.* 6.78-6.04 ppm assigned to O=C-NH-CH-, and oxazoline at *ca.* 7.50-7.08 ppm assigned to Ph-CH₂-oxazoline) with that of an end methyl group (S=C-CH₂-CH₃ at *ca.* 1.17-0.91 ppm) (see the corresponding ¹H NMR spectra in the ESI†). Number average molecular weight (*M*_n) and polydispersity index (PDI, *M*_w/*M*_n) of PN_xO_y were determined by gel permeation chromatography (GPC). Low PDI values (<1.10) suggests the narrow molecular weight distribution of PN_xO_y, which is crucial for successful single-chain folding.¹³ Fe^{II}-PN_xO_y formation was carried out in THF at 25 °C by using FeCl₂ as the iron(II) source. Feeding PN_xO_y precursor into the FeCl₂ solution at high dilution condition (0.16 mmol. mL⁻¹) prevented the unwanted interparticle coupling events during the single-chain folding.

**Scheme 2** Schematic representation of the synthesis of Fe^{II}-PN_xO_y (Fe^{II}-PN₁₂₀O₄, Fe^{II}-PN₁₅₀O₃, and Fe^{II}-PN₂₁₀O₃)**Scheme 3** Synthesis of Neat-C

To evaluate the importance of polymeric pockets around active sites, neat chiral Fe^{II} -oxazoline complex (denoted as Neat-C) was prepared as the control catalyst. As shown in Scheme 3, 4-benzyl-2-vinylloxazoline (5.0 mmol, 0.94 g) was dissolved in THF (20 mL). FeCl_2 (5.5 mmol, 0.70 g) in THF (50 mL) was added dropwise into the above solution under vigorous stirring. The mixture was stirred at room temperature for 10 h, and then concentrated in vacuum. Product was precipitated in cold *n*-pentane (100 mL). Filtration and drying in vacuum afforded the Neat-C as a brown powder.

Characterization of Samples

Cloud-point determination. Different from neat Fe^{II} -oxazoline complex (Neat-C) which is water-insoluble, Fe^{II} - PN_xO_y exhibits inverse temperature-dependent water-solubility due to the presence of thermosensitive NIPAAm unit. The cloud-point of Fe^{II} - PN_xO_y was measured by using UV-vis spectroscopy (Fig. 1A). It is the temperature at which the transmittance of corresponding aqueous solutions markedly decreased. Obviously, Fe^{II} - $\text{PN}_{120}\text{O}_4$, Fe^{II} - $\text{PN}_{150}\text{O}_3$, and Fe^{II} - $\text{PN}_{210}\text{O}_3$ presented cloud-point at *ca.* 26, 29 and 31 °C, respectively (Fig. 1A). Indeed, the nanoobjects were soluble in water at 25 °C (room temperature, lower than their cloud-point), while became hydrophobic gradually as local temperature increased (Fig. 1B). When the local temperature was up to 36 °C, they were completely precipitated out of water, as shown by the typical Fe^{II} - $\text{PN}_{150}\text{O}_3$ (Fig. 1B). Notably, the temperature for catalyst separation (36 °C) is slightly higher than room temperature (25 °C), which is a benefit for energy-saving in industrial applications. More interestingly, full reversibility without hysteresis was observed upon slow cooling (Fig. 1B). Such temperature-dependent dissolution-precipitation transitions behavior can be used to realize the coupling of the reaction and separation of Fe^{II} - PN_xO_y for asymmetric SMA in water.

UV-vis. The intramolecular Fe^{II} -oxazoline coordination in Fe^{II} - PN_xO_y was evaluated by UV-vis spectroscopy (Fig. 2A). Clearly, typical $\text{PN}_{150}\text{O}_3$ precursor exhibited a strong absorbed peak at 303 nm, which corresponded to $\pi \rightarrow \pi^*$ transitions of oxazoline group.¹⁴ After FeCl_2 treatment, the characteristic peak shifted to 297 nm, along with the appearance of a new peak at 497 nm which were assigned to Fe^{II} -oxazoline charge-transfer (Fig. 2A-a vs. 2A-b). It is convincing proof for the coordination of oxazoline to $\text{Fe}(\text{II})$ ion. To confirm the coordinate ability of oxazoline

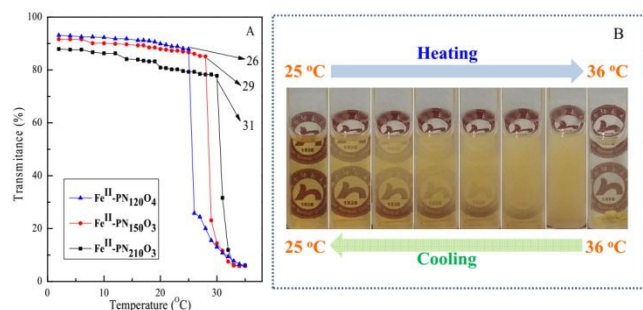


Fig. 1 (A) Transmittance curves of the Fe^{II} - PN_xO_y (Fe^{II} - $\text{PN}_{120}\text{O}_4$, Fe^{II} - $\text{PN}_{150}\text{O}_3$, and Fe^{II} - $\text{PN}_{210}\text{O}_3$) in aqueous solutions (concentration: 0.5 M); (B) aqueous solution of typical Fe^{II} - $\text{PN}_{150}\text{O}_3$ at local temperature range from 25 to 36 °C

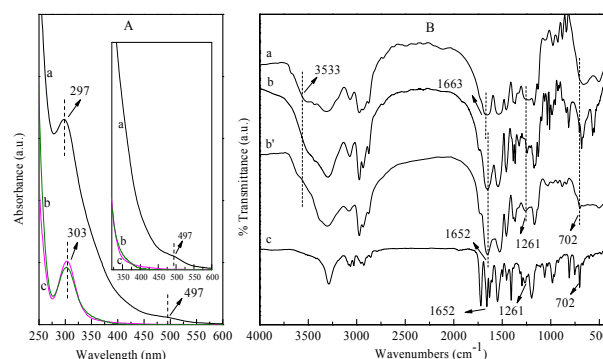


Fig. 2 (A) UV-vis spectra of $\text{PN}_{150}\text{O}_3$ (a), Fe^{II} - $\text{PN}_{150}\text{O}_3$ (b) and HCl-treated Fe^{II} - $\text{PN}_{150}\text{O}_3$ (c); (B) FT-IR spectra of $\text{PN}_{150}\text{O}_3$ (a), fresh Fe^{II} - $\text{PN}_{150}\text{O}_3$ (b), recovered Fe^{II} - $\text{PN}_{150}\text{O}_3$ after the 7th reuse (b') and Neat-C (c).

group, oxazoline in $\text{PN}_{150}\text{O}_3$ was protonated with HCl before it was exposed to $\text{Fe}(\text{II})$ ion. Indeed, the protonated $\text{PN}_{150}\text{O}_3$ failed to coordinate with $\text{Fe}(\text{II})$ ion, as evident from the absence of Fe^{II} -oxazoline charge-transfer peak (at 497 nm) (Fig. 2A-c).

FT-IR. Additional information on the metal coordination can be obtained from the FT-IR spectroscopy (Fig. 2B). Obviously, parent $\text{PN}_{150}\text{O}_3$ exhibited the characteristic C=N stretching vibration of oxazoline at 1663 cm^{-1} (Fig. 2B-a).¹⁵ The stretching vibration shifted to 1652 cm^{-1} when $\text{PN}_{150}\text{O}_3$ was treated with FeCl_2 (Fig. 2B-b vs. 2B-a). It gives an evidence for the participation of C=N group in forming coordination bonds with $\text{Fe}(\text{II})$ ion. Indeed, a characteristic N-Fe stretching vibration was observed at 702 cm^{-1} in FT-IR spectrum of Fe^{II} - $\text{PN}_{150}\text{O}_3$ (Fig. 2B-b).¹⁶ The formation of N-Fe dative bonds should operate as triggers for the self-folding of $\text{PN}_{150}\text{O}_3$, enabling the creation of an enclosed polymeric pocket around $\text{Fe}(\text{II})$ ions. The heteroatom of oxygen in oxazoline don't take part in the coordination as evident from the intact C-O-C band (at 1261 cm^{-1}) during the treatment with $\text{Fe}(\text{II})$ ion (Fig. 2B-b vs. 2B-a).¹⁵ Notably, the characteristic bands associated with Fe^{II} -oxazoline in Fe^{II} - $\text{PN}_{150}\text{O}_3$ are similar to those of Neat-C (Fig. 2B-b vs. 2B-c). It suggests the identity of catalytic Fe^{II} -oxazoline sites in Fe^{II} - PN_xO_y with Neat-C. Apart from the characteristic vibration associated with Fe^{II} -oxazoline complex, additional band at around 3533 cm^{-1} was also obvious in the FT-IR spectrum of Fe^{II} - $\text{PN}_{150}\text{O}_3$ (Fig. 2B-b vs. 2B-c). It is associated with stretching vibration mode of N-H of amide group in the thermo-responsive NIPAAm moiety.¹⁷ Notably, no change in the amide band was observed during the incorporation of $\text{Fe}(\text{II})$ ion into $\text{PN}_{150}\text{O}_3$, which means that the thermo-sensitive NIPAAm remained intact during the coordination (Fig. 2B-b vs. 2B-a). Therefore, $\text{Fe}(\text{II})$ ions are only shielded in the oxazoline cavity *via* metal-coordination. The hydrophobic shielding of active site, together with the coordination sphere provided by folded copolymer, makes these Fe^{II} -containing SCPNs structurally similar to metalloenzyme.

Job's plot analysis. The binding stoichiometry of $\text{Fe}(\text{II})$ ion to oxazoline in Fe^{II} - PN_xO_y was determined by using Job's method, an approach that determined the stoichiometry of chemical equilibria (Fig. 3).^{8c,18} In this method, UV-vis absorbance of $\text{Fe}(\text{II})$ -oxazoline complex which is proportional to the complex

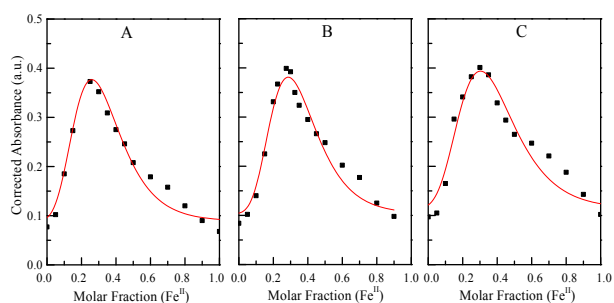


Fig. 3 Job's plot to determine the binding stoichiometry of Fe(II) ions. PN₁₂₀O₄ (A), PN₁₅₀O₃ (B) and PN₂₁₀O₃ (C) with Fe^{II} obtained from variations in absorption at 297 nm

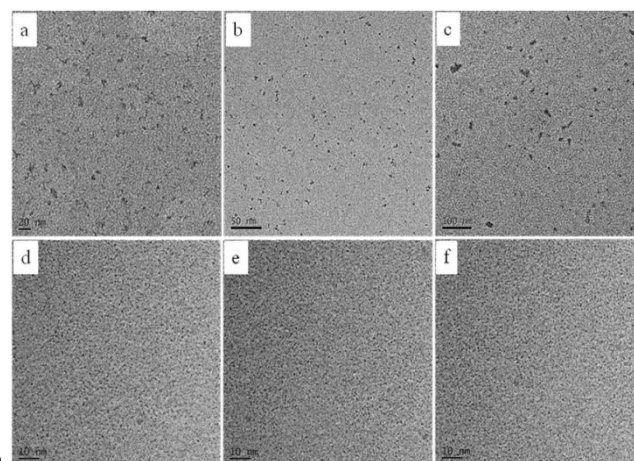


Fig. 4 TEM images of PN₁₅₀O₃ (a), Fe^{II}-PN₁₅₀O₃ (b), and HCl-treated Fe^{II}-PN₁₅₀O₃ (c) in methanol, as well as the Fe^{II}-PN₁₂₀O₄ (d), Fe^{II}-PN₁₅₀O₃ (e) and Fe^{II}-PN₂₁₀O₃ (f) in water at room temperature stained with phosphotungstic acid

concentration was plotted against the mole fraction of Fe(II) ion, while the total concentration of FeCl₂ and oxazoline was kept constant. The obtained Job's plots of Fe^{II}-PN₁₂₀O₄, Fe^{II}-PN₁₅₀O₃, and Fe^{II}-PN₂₁₀O₃ gave the maximum points at the Fe(II) mole fraction of 0.26, 0.29 and 0.3, respectively. Actually, the values represent mole fractions of Fe(II) ion in corresponding metal-coordination chemical equilibrium. According to the Job's plot, we estimated that the average coordination of oxazoline to Fe(II) ion in Fe^{II}-PN₁₂₀O₄, Fe^{II}-PN₁₅₀O₃, and Fe^{II}-PN₂₁₀O₃ was about 2.8, 2.4, and 2.3, respectively. The average coordination numbers are accorded with the numbers of oxazoline units per polymer chain. It suggests the intrachain metal coordination for Fe^{II}-PN_xO_y, rather than interchain coupling. Polymer backbone together with hydrophilic NIPAAm shell should isolate the oxazoline units, preventing interchain coupling events. Notably, the binding stoichiometry in Fe^{II}-PN_xO_y is less than the theoretical coordination number of Fe(II) ions (*i.e.*, 6 for an octahedron coordination). The unsaturated iron sites may favor the coordination of carbonyl oxygen in α,β -unsaturated ketones to Fe(II) center, which increases the electrophilicity of the β -carbon and assisted the conjugate addition.¹⁹ Furthermore, the vacant coordination site on Fe(II) core should also benefit the formation of the Fe-thiol complex. This pre-coordinated thiol may play a role in orienting or activating the enone acceptor within the Fe-oxazoline complex through the known *trans* directing effect of sulfur ligands in metal complexes.^{5,20}

TEM. The intrachain Fe^{II}-oxazoline coordination that triggers the self-folding of individual polymer chains simultaneously was further confirmed by TEM (Fig. 4). Clearly, PN₁₅₀O₃ precursor was unfolded in methanol, a good solvent for the both PNIPAAm and oxazoline segments, adopting a random coil conformation in the TEM image (Fig. 4a). Being treated with Fe(II) ion, the copolymer chain coiled into nanoparticles with an ultrasmall size in the range of 4–10 nm (Fig. 4b). This diameter value of obtained Fe^{II}-PN₁₅₀O₃ is consistent with that adopting a single-chain folded conformation in solution.^{8c,21} Notably, HCl-treated PN₁₅₀O₃ failed to fold in methanol even through it was exposed to Fe(II) ions (Fig. 4c). This is attributed to the loss of coordinate ability of oxazoline group in PN₁₅₀O₃, as confirmed by UV-vis spectra (Fig. 2A–c). These observations confirm the intramolecular folding upon Fe^{II}-oxazoline coordination. Instead of the random coil morphologies in methanol, Fe^{II}-PN₁₅₀O₃ adopted more compact globule conformation in water (a good solvent for PNIPAAm, but bad solvent for oxazoline) at room

temperature (Fig. 4e). The size of Fe^{II}-PN₁₅₀O₃ decreased to *ca.* 1.0 nm when water was used as the solvent. It is indicative of the intramolecular hydrophobic interaction which makes the SCPNs more compact. Similar morphologies were observed for the Fe^{II}-PN₁₂₀O₄ and Fe^{II}-PN₂₁₀O₃ in water (Fig. 4d and 4f). The observations confirm that amphiphilic PN_xO_y self-fold in water through the cooperation of intrachain metal coordination and hydrophobic interaction. The resulted Fe^{II}-PN_xO_y should adopt an individual core-shell nanostructure with the hydrophobic Fe^{II}-oxazoline core surrounded by hydrophilic PNIPAAm shell. Such morphology is akin to the globular, native conformation of enzymes which showed a hydrophobic core and a hydrophilic shell in aqueous media.²²

Particle size distribution analysis. Dynamic light scattering (DLS) was employed to further determine the hydrodynamic diameter (D_h) and size distribution of PN₁₅₀O₃ and Fe^{II}-folded SCPNs in water at 25 °C (Fig. 5). Clearly, the typical PN₁₅₀O₃ has a D_h of 15.9 nm in water, while the D_h of Fe^{II}-PN₁₅₀O₃ reduced to 8.7 nm. These findings confirm the intramolecular folding upon Fe-oxazoline coordination. Indeed, all Fe^{II}-PN_xO_y formed aggregates in water with D_h in the range of 7.5–13.5 nm, indicative of the intramolecular chain collapse. Interestingly, the size of Fe^{II}-PN_xO_y in water gradually decreased with increasing the hydrophobic oxazoline content. D_h of Fe^{II}-PN₂₁₀O₃, Fe^{II}-PN₁₅₀O₃, and Fe^{II}-PN₁₂₀O₄ were *ca.* 13.5, 8.7, and 7.5 nm, respectively. This tendency is fully consistent with the fact that intrachain hydrophobic interaction of oxazoline made the Fe^{II}-folded PN_xO_y compact. These observations give further evidence for the intramolecularly self-folding of Fe^{II}-PN_xO_y as a result of the cooperation of intrachain metal complexation and hydrophobic forces. The concurrent binding/folding strategy makes the Fe^{II}-containing SCPNs uniform and compact in water, as evidenced by the polydispersity indexes (PDI). Obviously, the hydrodynamic diameter analysis gave low PDI values for Fe^{II}-PN₁₂₀O₄, Fe^{II}-PN₁₅₀O₃, and Fe^{II}-PN₂₁₀O₃ (0.283, 0.312, and 0.275, respectively), suggesting the homogeneous distribution, spherical morphology, and uniform size of the corresponding SCPNs.^{17,23} Aggregation of the resulting SCPNs should be prevented by the steric repulsion of multiple hydrophilic

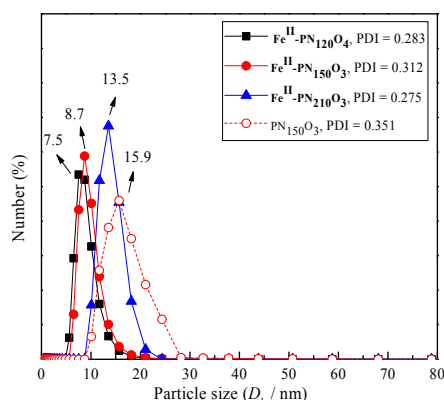


Fig. 5 Size distribution of $\text{Fe}^{\text{II}}\text{-PN}_x\text{O}_y$ and $\text{PN}_{150}\text{O}_3$ in water at room temperature (concentration of 0.5 mg mL^{-1})

PNIPAAm chains which isolated a single main chain in water. The PDI value of $\text{PN}_{150}\text{O}_3$ in water was relatively higher (0.351), probably due to the sparse morphology. These observations are in complete agreement with the results obtained in TEM images.

Catalytic Performances

As expected, Fe^{II} -folded SCPNs provided the hydrophobic reaction spaces to accommodate asymmetric SMA of propanethiol to chalcone in water. As shown in Table 1, the asymmetric conjugation addition proceeded efficiently in water with the employment of $\text{Fe}^{\text{II}}\text{-PN}_x\text{O}_y$ (Table 1, entries 1-4). In particular, only 3 mol% of $\text{Fe}^{\text{II}}\text{-PN}_{150}\text{O}_3$ was sufficient to afford almost quantitative yield (95%) of the Michael adduct with excellent enantioselectivity (96%) (Table 1, entry 2). The absolute configuration of product was assigned to be (*S*) by comparing with the optical rotation value reported in the literature.^{5a} However, in the absence of polymer frameworks, neat Fe^{II} -oxazoline complex (Neat-C) was far less active and selective for this transformation. Low yield (43%) with disappointing ee value (83%) was obtained under identical conditions (Table 1, entry 5). The discrepancy in catalytic efficiency emphasizes an importance of the catalytic, hydrophobic compartment for the aqueous catalysis. Apart from hydrophobic shielding of Fe^{II} -oxazoline from the aqueous environment, the hydrophobic compartment effectively sequestered substrates from the surrounding water through hydrophobic attractive forces.^{8d,17,24} The high local concentration of substrates around catalytic sites in the interior of Fe^{II} -folded SCPNs allowed us to use low catalyst loading for efficient catalysis. More importantly, the internal chirality of hydrophobic compartment should further induce the confined asymmetric catalysis, introducing highly enantioselective effects.^{22b} Interestingly, midway addition of $\text{PN}_{150}\text{O}_3$ copolymer (equivalent to the $\text{PN}_{150}\text{O}_3$ amount in $\text{Fe}^{\text{II}}\text{-PN}_{150}\text{O}_3$) into the Neat-C system failed to improve the catalytic efficiency (Table 1, entry 6 vs. 5). It is reasonable that unlike the organic substrates, the water-insoluble Neat-C is solid, and gives a small amount in solution, it is hard to be encapsulated in the hydrophobic domain along with substrates. The results are agree with our hypothesis that high local concentration of substrates around catalytic sites is crucial for this system to be active, and this is only achieved in the presence of hydrophobic, catalytic compartments.

Table 1 Results of asymmetric SMA of thiols to α , β -unsaturated ketones in water with chiral Fe^{II} -oxazoline catalysts ^a

$\text{R}_1\text{-CH=CH-C(=O)R}_2 + \text{R}_3\text{-SH} \xrightarrow[\text{Water, 25 } ^\circ\text{C}]{\text{Cat (3.0 mol\%)}} \text{R}_1\text{-CH(SR}_3\text{)-CH}_2\text{-C(=O)R}_2 \quad (I-9)$								
Entry	Catalyst	R ₁	R ₂	R ₃	Product	T (h)	Yield ^b (%)	ee ^c (%)
1	Fe^{II}-PN₁₂₀O₄					36	88	99
2	Fe^{II}-PN₁₅₀O₃					36	95	96
3	Fe^{II}-PN₁₅₀O₃ ^d	Ph	Ph	<i>n</i> -C ₃ H ₇	1	48	92	94
4	Fe^{II}-PN₂₁₀O₃					36	91	96
5	Neat-C					36	43	83
6	Neat-C ^e					36	47	82
7	Fe^{II}-PN₁₅₀O₃	Ph	CH ₃	<i>n</i> -C ₃ H ₇	2	24	96	99
8	Neat-C					24	59	70
9	Fe^{II}-PN₁₅₀O₃	4-	Ph	<i>n</i> -C ₃ H ₇	3	48	92	98
10	Neat-C	OMePh				48	46	60
11	Fe^{II}-PN₁₅₀O₃	4-	CH ₃	<i>n</i> -C ₃ H ₇	4	48	95	90
12	Neat-C	OMePh				48	51	67
13	Fe^{II}-PN₁₅₀O₃	4-NO ₂ Ph	Ph	<i>n</i> -C ₃ H ₇	5	48	10	89
14	Neat-C					48	3	59
15	Fe^{II}-PN₁₅₀O₃	Ph	Ph	4-Cl-C ₆ H ₄ -CH ₂	6	36	93	95
16	Neat-C					36	56	87
17	Fe^{II}-PN₁₅₀O₃	4-	Ph	4-Cl-C ₆ H ₄ -CH ₂	7	48	90	96
18	Neat-C	OMePh				48	54	90
19	Fe^{II}-PN₁₅₀O₃	CH ₃	CH ₃	4-Cl-C ₆ H ₄ -CH ₂	8	48	94	>99
20	Neat-C					48	52	69
21	Fe^{II}-PN₁₅₀O₃	Ph	Ph	4-Cl-C ₆ H ₄	9	48	92	98
22	Neat-C					48	68	55

^a Catalyst (3.0 mol% of ketones, based on iron content), α , β -unsaturated ketones (0.1 mmol), thiol (0.12 mmol), water (1.0 mL), 25 °C.

^b Isolated yield after column chromatography.

^c Determined by HPLC (Daicel Chiralpak AD column). The absolute configuration of product was assigned to be (*S*) by comparing with the optical rotation value reported in the literature.^{5a}

^d Catalyst (3.0 mol% of ketones, based on iron content), α , β -unsaturated ketones (4.0 mmol), thiol (5.0 mmol), water (20 mL), 25 °C.

^e Neat-C (3.0 mol% of chalcone, based on iron content), $\text{PN}_{150}\text{O}_3$ (0.061 g, equivalent to the amount of $\text{PN}_{150}\text{O}_3$ in $\text{Fe}^{\text{II}}\text{-PN}_{150}\text{O}_3$), chalcone (0.1 mmol), propanethiol (0.12 mmol), water (1.0 mL), 25 °C.

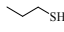
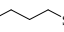
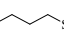
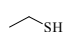
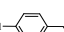

Since compartmentalized SCPNs behaved as a catalytic nanoreactor for asymmetric SMA reaction, morphology and microenvironment of the hydrophobic compartment directly affected the catalytic activity of $\text{Fe}^{\text{II}}\text{-PN}_x\text{O}_y$. Indeed, $\text{Fe}^{\text{II}}\text{-PN}_{150}\text{O}_3$ -based SCPNs with D_h of 8.7 nm showed the highest catalytic efficiency in aqueous asymmetric SMA of propanethiol to chalcone (Table 1, entry 2). It could even mediate the gram-scale SMA reaction smoothly, yielding large quantity of (*S*)-3-(propylthio)-1,3-diphenylpropan-1-one (1.12 g, 92% yield) with excellent ee value (94% ee) (Table 1, entry 3). Reduced size of the SCPNs ($\text{Fe}^{\text{II}}\text{-PN}_{120}\text{O}_4$, D_h = 7.5 nm) was unfavorable for the transformation (Table 1, entry 1), probably due to the limited mobility of substrates in the catalytic pocket. Furthermore,

conformational freedom of Fe^{II}-oxozaline complexes should be also limited in the smaller compartment, which was undesirable for the asymmetric catalysis. While, **Fe^{II}-PN₂₁₀O₃** which folded into larger SCPNs (*D_h* = 13.5 nm) was also detrimental to the catalysis (Table 1, entry 4). Too dense chain loops around the metal-ions, which blocks access of substrate to the catalytic pockets, may result in the decline in activity.^{8d} The observations provide further evidence for the confined catalysis in the SCPN compartment.

Different from natural metalloenzymes which often exhibits a narrow substrate range, the **Fe^{II}-PN₁₅₀O₃** is universal in the aqueous asymmetric SMA. A wide range of α , β -unsaturated ketones, ether aromatic or aliphatic, get almost quantitatively conjugate addition to yield the corresponding adducts (90-96%) with excellent enantioselectivity (90-99%) in water although they were water-incompatible (Table 1, entries 7, 9, 11, 15, 17, 19 and 21). Poor yield (10%) was observed over the nitro-substituted ketones, despite the encouraging enantioselectivity (89%) (Table 1, entry 13). The lower reactivity is probably due to undesirable competitive complexation of the nitro group to Fe(II) center,²⁵ which retards the precoordination of thiol to Fe(II) center for the conjugate addition. Furthermore, the nitro group in 4-nitrochalcone decreases the electron density at the carbonyl oxygen by inductive and resonance effects, which may further weaken the coordination between carbonyl oxygen and Fe(II) center. Interestingly, the use of benzyl mercaptan as sulfur source still provided the desired chiral β -thioketones with high yield (90-94%) and ee values (95-99%), although the nucleophile was more sterically demanding (Table 1, entries 15, 17 and 19). Furthermore, 4-chlorobenzenethiol, a less reactive nucleophile, also reacted with chalcone smoothly to afford the β -keto sulfide **9** in 92% yield and 98% ee value (Table 2, entry 21). In all cases, no disulfide formation was observed in water medium. Using the different alkyl thiols affords the access to optically active chiral sulfur compounds bearing removable S-protecting groups.²⁶

Benefiting from the hydrophobic, catalytic compartment, the Fe^{II}-folded SCPNs were superior to other reported catalytic systems either metallic or organic, such as per-6-amino- β -cyclodextrin,²⁷ Sc(OTf)₃/bipyridine,²⁸ cinchona alkaloid-squaramide,^{2b} and Fe^{III}-salen complex,^{5a} as seen in Table 2. At room temperature, only 3.0 mol% of **Fe^{II}-PN₁₅₀O₃** was sufficient to efficiently catalyze the asymmetric SMA reaction in water without the use of any additives, due to the hydrophobic shielding effective and synergistic effect of metal center with polymeric framework (Table 2, entry 1). Despite possessing similar hydrophobic cavities, β -cyclodextrin was far less selective. Stoichiometric per-6-amino- β -cyclodextrin catalyst was insufficient to provide the β -adduct with satisfied ee value, although the yield was encouraging (Table 2, entry 2).²⁵ Sc(OTf)₃/bipyridine, a Lewis acid catalytic system, could catalyze this transformation in an enantioselective fashion (Table 2, entry 3). But it suffered from low catalytic activity due to the poor water-solubility of catalysts and substrates. Furthermore, strong base of sodium hydroxide was required in the Sc(OTf)₃/bipyridine system to ensure the conversion to Michael adduct, which was undesirable for industrial application (Table 2, entry 3).²⁷ Cinchona alkaloid-squaramide employing hydrogen bond for substrate activation circumvented the undesirable

Table 2 Asymmetric conjugate addition of various thiols to chalcone over different catalysts

Entry	Catalyst	Catalyst loading ^f	Nucleophile	Solvent	<i>T</i> (h)	Yield ^b (%)	ee ^c (%)
1	Fe^{II}-PN₁₅₀O₃ ^a	3.0 mol%		H ₂ O	24	95	96
2	Per-6-amino- β -cyclodextrin ^b	100 mol%		H ₂ O	36	100	23
3	Sc(OTf) ₃ /bipyridine ^c	1.0 mol%		H ₂ O	70	64	83
4	Cinchona alkaloid-squaramide ^d	1.0 mol%		Toluene	24	80	96
5	Fe^{II}-PN₁₅₀O₃ ^a	3.0 mol%		H ₂ O	36	93	95
6	Fe ^{III} -salen complex ^e	10 mol%		CH ₂ Cl ₂	36	68	84

^a **Fe^{II}-PN₁₅₀O₃** (0.003 mmol), chalcone (0.1 mmol), thiol (0.12 mmol), water (1.0 mL), 25 °C (In this work)

^b Per-6-amino- β -cyclodextrin (0.1 mmol), chalcone (0.1 mmol), thiol (0.1 mmol), water (1.0 mL), 25 °C (Ref. 27).

^c Sc(OTf)₃ (0.005 mmol), bipyridine (0.01 mmol), chalcone (0.5 mmol), thiol (0.5 mmol), NaOH (3.0-20.0 mol %, the minimum quantity to reach pH = 7.0), water (1.0 mL), 30 °C (Ref. 28).

^d Cinchona alkaloid-squaramide catalyst (0.0025 mmol), chalcones (0.25 mmol), thiol (0.375 mmol), toluene (1.0 mL), 25 °C (Ref. 2b).

^e Fe^{III}-salen (0.01 mmol), chalcone (0.1 mmol), thiol (0.12 mmol), CH₂Cl₂ (1.0 mL), 25 °C (Ref. 5a).

^f The mol% of chalcone.

^g Isolated yield after column chromatography.

^h Determined by HPLC (Daicel Chiralpak AD column).

additives in the enantioselective SMA.^{2b} Nevertheless, non-polar organic solvents, such as toluene and dichloromethane, were required to ensure the efficiency.^{2b} If water is used as the reaction medium, low enantioselectivity or even racemic product should be detected due to the competition for the hydrogen bond of water with the catalyst (Table 2, entry 4).^{2b} Furthermore, the **Fe^{II}-PN₁₅₀O₃** in water was even more efficient than other reported iron-based complex in organic solvent (Table 2, entry 5 vs. 6). The 10 mol% of reported chiral Fe^{III}-salen catalyst gave only 68 % yield of (*R*)- β -keto sulfide with low enantioselectivity (84%) even though the addition was performed in dichloromethane (Table 2, entry 6).^{5a} The results demonstrate the advantages of metalloenzyme mimicking Fe^{II}-folded SCPNs used for asymmetric SMA reaction in water.

90 Reusability

Apart from exhibiting superior activity and selectivity, **Fe^{II}-PN_xO_y** exhibited the thermal driven “smart” recovery in the aqueous system due to the presence of thermo-sensitive PNIPAAm shell. After reaction, the Fe^{II}-folded SCPNs turned hydrophobic upon heating above their corresponding cloud-point (Fig. 1). This allows for their separation from aqueous phase by decantation. To our delight, the recovered catalysts of **Fe^{II}-PN₁₂₀O₄**, **Fe^{II}-PN₁₅₀O₃** and **Fe^{II}-PN₂₁₀O₃** could be reused up to seven times without significant loss in activity and selectivity in asymmetric SMA of propanethiol to chalcone in water (Fig. 6A). Leaching of Fe(II) species, a main reason for deactivation of the iron-containing catalyst, did not occur during the addition, as

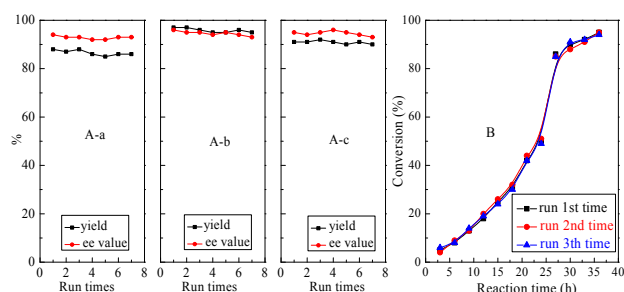


Fig. 6 (A) Reuse of $\text{Fe}^{\text{II}}\text{-PN}_{120}\text{O}_4$ (a), $\text{Fe}^{\text{II}}\text{-PN}_{150}\text{O}_3$ (b) and $\text{Fe}^{\text{II}}\text{-PN}_{210}\text{O}_3$ (c) in asymmetric SMA reaction of propanethiol to chalcone in water, (B) kinetic curves of the consecutive experimental runs 1-3 over $\text{Fe}^{\text{II}}\text{-PN}_{150}\text{O}_3$

proved by the leaching tests of recovered catalysts by ICP. Indeed, chemical analysis of the recovered catalysts gave the iron content (0.089, 0.067, and 0.044 mmol g^{-1} for recovered $\text{Fe}^{\text{II}}\text{-PN}_{120}\text{O}_4$, $\text{Fe}^{\text{II}}\text{-PN}_{150}\text{O}_3$ and $\text{Fe}^{\text{II}}\text{-PN}_{210}\text{O}_3$, respectively) almost identical to that of the corresponding fresh one. The negligible leaching of catalysts should arise from the hydrophobic shielding of Fe^{II} -oxazoline complex in a structured compartment which protected by PNIPAAm shell. Excellent stability of the $\text{Fe}^{\text{II}}\text{-PN}_x\text{O}_y$ is also evident from the FT-IR spectra of typical $\text{Fe}^{\text{II}}\text{-PN}_{150}\text{O}_3$ with fresh and reused seven times (Fig. 2b vs. b'). Kinetics study provided the other substantial proof for the stability of $\text{Fe}^{\text{II}}\text{-PN}_x\text{O}_y$, based on the fact that no significant change in the apparent rate constant occurred in the consecutive experimental runs 1-3 over typical $\text{Fe}^{\text{II}}\text{-PN}_{150}\text{O}_3$ (Fig. 6B).²⁹ The facile recovery together with the perfect stability makes $\text{Fe}^{\text{II}}\text{-PN}_x\text{O}_y$ highly promising in sustainable industrial applications.

Conclusions

In conclusion, Fe^{II} -folded SCPNs which shielded chiral Fe^{II} -oxazoline complex in a hydrophobic compartment have been constructed through the cooperation of intrachain Fe^{II} -oxazoline coordination and hydrophobic interaction. These synthetic soft nanoentities mimic the compartmentalized structure and catalytic function of metalloenzyme, allowing efficient asymmetric SMA of thiols to a wide range α , β -unsaturated ketones in water at room temperature without the need of any organic solvent or additional additives. In particular, they can be readily recovered from the aqueous system for efficient reuse by simply adjusting the local temperature. The novel catalytic system offers several advantages, such as operational simplicity, mild reaction conditions, low catalyst loading, high efficiency, and facile reuse of catalyst. All these advantages make it a benign protocol from the sustainability point of view, and inspired us to design the other enzyme mimics for a wide range of sustainable industrial applications.

Experimental Section

Materials and Reagents

L-phenylalaninol, acryloylchloride and *p*-toluenesulfonyl chloride (TsCl) were brought from Aldrich. 4-(Dimethylamino) pyridine (DMAP) and *p*-anisaldehyde were purchased from MACKLIN. *P*-nitrobenzaldehyde, propanethiol, 4-chlorobenzylthiophenol, 4-chlorobenzenethiol, and 3-penten-2-one were obtained from J&K. AIBN,

FeCl_2 and acetophenone were brought from Alfa Aesar. NIPAAm was purchased from Acros. Other commercially available chemicals were laboratory grade reagents from local suppliers. AIBN was recrystallized from methanol. All reagents used for the monomer synthesis were stirred over CaH_2 , freshly distilled under vacuum, and kept under a dry argon atmosphere until use.

Methods

FT-IR spectra were obtained as potassium bromide pellets with a resolution of 4 cm^{-1} and 64 scans in the range of 400–4000 cm^{-1} using an AVATAR 370 Thermo Nicolet spectrophotometer. NMR spectra were recorded on a BRUKER AVANCE-500 spectrometer with TMS as an internal standard. Iron contents in catalysts were determined by inductively coupled plasma mass spectrometry (ICP-MS) on a NexION 300X analyzer (Perkin-Elmer Corp.). Optical rotation of samples was measured on a WZZ-2A Automatic Polarimeter. Molecular weight and the molecular weight distribution of copolymers were obtained by GPC. Analyses were performed on an Alltech Instrument (Alltech, America) using THF as the solvent eluting at a flow of 1.0 mL min^{-1} through a Jordi GPC 10000 A column (300 mm \times 7.8 mm) equipped with an Alltech ELSD 800 detector. Cloud-point of catalysts in water was determined by measuring the transmittance of the corresponding aqueous solution (0.5 mg. mL^{-1}) using a UV-visible photometer. Morphologies of Fe^{II} -folded SCPNs were observed by TEM on a Microscope JEM-2100F at an accelerating voltage of 200 kV. Samples were prepared by depositing the aqueous solution (0.5 mg. mL^{-1}) onto an ultrathin carbon-coated copper grid, followed by removal of excess solution by blotting the grid with filter paper. The samples were dried for 48 h at room temperature in desiccators and were negatively stained by phosphotungstic acid. Hydrodynamic diameter (D_h) of Fe^{II} -folded SCPNs was determined by DLS using a MS2000 Laser Particle Size Analyzer (Malvern, U.K.). The aqueous solution of samples (0.5 M) was filtered through a 0.45 μm disposable polyamide membrane to free it from dust particles before measurement.

Preparation of $\text{Fe}^{\text{II}}\text{-PN}_x\text{O}_y$ ($x=120, y=4$; $x=150, y=3$; $x=210, y=3$)

Synthesis of 4-benzyl-2-vinyloxazoline: *L*-phenylalaninol (9.0 mmol, 1.36 g) and triethylamine (9.2 mmol, 0.93 g) were dissolved in dichloromethane (10 mL), and then cooled to 0 $^{\circ}\text{C}$. Acryloyl chloride (9.2 mmol, 0.83 g) in dichloromethane (10 mL) was added dropwise over 1 h at 0 $^{\circ}\text{C}$. The mixture was stirred at room temperature for 15 h, and then was extracted with saturated brine (3 \times 15 mL). After being dried over anhydrous Na_2SO_4 , organic phase was mixed with DMAP (0.8 mmol, 0.10 g) and triethylamine (8.2 mmol, 0.83 g) at 0 $^{\circ}\text{C}$. TsCl (8.0 mmol, 1.53 g) in dichloromethane (10 mL) was then added. The mixture was stirred at room temperature for 12 h. The obtained solution was washed with saturated NH_4Cl (3 \times 10 mL) to remove the DMAP, and further washed with saturated NaHCO_3 (3 \times 10 mL) to remove the formed hydrochloric acid. Organic layer was dried over anhydrous Na_2SO_4 . After being concentrated in vacuum, the residue was purified by chromatography on basic alumina with petroleum ether/ethyl acetate ($v/v=1/1$), giving 4-benzyl-2-vinyloxazoline as the white powder (0.88 g, yield: 59%). FT-IR (KBr): $\gamma_{\text{max}}/\text{cm}^{-1}$ 3418, 3290, 3084, 3032, 2972, 2929, 2790, 1720, 1663, 1629, 1549, 1409, 1299, 1262, 1207, 1108, 1061, 1033, 983, 924, 885, 808, 752, 705, 603, 567, 477. ^1H NMR (500 MHz, CDCl_3): δ (ppm): 7.34–7.22 (m, 5 H, *Ph*- CH_2 -oxazoline), 6.30–5.90 (m, 3 H, $\text{CH}_2=\text{CH}$ -oxazoline), 4.25–4.23 (m, 1 H, O- CH_2 -CH-N in oxazoline),

4.22-4.16 (m, 2 H, O-CH₂-CH-N in oxazoline), 3.03-2.86 (m, 2 H, Ph-CH₂-oxazoline).

Synthesis of PN_xO_y: A certain feed molar ratio of NIPAAm and oxazoline (10 mmol of NIPAAm and 0.33 mmol of oxazoline for PN₁₂₀O₄, 10 mmol of NIPAAm and 0.2 mmol of oxazoline for PN₁₅₀O₃, 10 mmol of NIPAAm and 0.14 mmol of oxazoline for PN₂₁₀O₃) were dissolved in anhydrous methanol (15 mL) in Schlenk tube. AIBN (1/80 of the total molar of monomers) and benzyl dithiopropionate (1/80 of the total molar of monomers) were then added as the radical initiator and chain transfer agent, respectively, for this copolymerization. The solutions were degassed by three freeze-pump-thaw cycles to remove oxygen completely. Polymerizations were carried out at 60 °C under dry argon atmosphere. After 24 h, the solutions were cooled with liquid nitrogen to cease the reactions, and then were concentrated in vacuo. Crude products were dissolved in THF (5.0 mL), and subsequently precipitated for three times from diethyl ether (100 mL). After being dried in vacuum, the copolymers were obtained as light yellow powder, which were denoted as PN_xO_y (x=120, y= 4; x=150, y= 3; x= 210, y= 3, the numbers of NIPAAm and oxazoline units were determined by ¹H NMR spectra of corresponding copolymer).

PN₁₂₀O₄: FT-IR (KBr): $\gamma_{\text{max}}/\text{cm}^{-1}$ 3533, 3440, 3310, 3068, 2973, 2946, 2892, 1663, 1538, 1458, 1368, 1342, 1261, 1172, 1131, 1079, 977, 927, 880, 838, 660, 504. ¹H NMR (500 MHz, CDCl₃): δ (ppm): 7.39-7.08 (m, 25 H, Ph-CH₂-oxazoline and Ph-CH₂-CH₂-CH- in backbone chain), 6.59-6.27 (m, 120 H, O=C-NH-CH in NIPAAm), 4.01-3.89 (m, 126 H, -CH-CH₂- of backbone chain in NIPAAm, -CH-CH₂- of backbone chain in oxazoline and S=C-CH₂-CH₃ in backbone chain), 3.78-2.03 (m, 248 H, -CH-CH₂- of backbone chain in NIPAAm and -O-CH₂-CH-N- in oxazoline), 1.89-1.57 (m, 130 H, CH₃-CH-CH₃ in NIPAAm, Ph-CH₂-oxazoline, -O-CH₂-CH-N- in oxazoline and Ph-CH₂-CH₂-CH- in backbone chain), 1.45-1.38 (m, 8 H, -CH-CH₂- of backbone chain in oxazoline), 1.28-1.16 (m, 720 H, CH₃-CH-CH₃ in NIPAAm), 0.91-0.88 (m, 3 H, S=C-CH₂-CH₃ in backbone chain). GPC (THF): *M_n* = 14456, *M_w* = 15178, PDI = 1.05.

PN₁₅₀O₃: FT-IR (KBr): $\gamma_{\text{max}}/\text{cm}^{-1}$ 3533, 3438, 3312, 3068, 2974, 2945, 2897, 1663, 1542, 1460, 1367, 1340, 1261, 1172, 1129, 1068, 981, 934, 876, 838, 663, 505. ¹H NMR (500 MHz, CDCl₃): δ (ppm): 7.50-7.08 (m, 20 H, Ph-CH₂-oxazoline and Ph-CH₂-CH₂-CH- in backbone chain), 6.78-6.04 (m, 150 H, O=C-NH-CH in NIPAAm), 4.77-4.02 (m, 154 H, -CH-CH₂- of backbone chain in NIPAAm, -CH-CH₂- of backbone chain in oxazoline and S=C-CH₂-CH₃ in backbone chain), 2.97-2.55 (m, 306 H, -CH-CH₂- of backbone chain in NIPAAm and -O-CH₂-CH-N- in oxazoline), 2.23-2.17 (m, 158 H, CH₃-CH-CH₃ in NIPAAm, Ph-CH₂-oxazoline, -O-CH₂-CH-N- in oxazoline, and Ph-CH₂-CH₂-CH- in backbone chain), 2.08-1.88 (m, 6 H, -CH-CH₂- of backbone chain in oxazoline), 1.29-1.67 (m, 900 H, CH₃-CH-CH₃ in NIPAAm), 1.17-0.91 (m, 3 H, S=C-CH₂-CH₃ in backbone chain). GPC (THF): *M_n* = 17328, *M_w* = 18735, PDI = 1.08.

PN₂₁₀O₃: FT-IR (KBr): $\gamma_{\text{max}}/\text{cm}^{-1}$ 3533, 3437, 3310, 3071, 2977, 2949, 2897, 1663, 1540, 1459, 1368, 1341, 1261, 1172, 1133, 1075, 979, 930, 879, 841, 662 504. ¹H NMR (500 MHz, CDCl₃): δ (ppm): 7.29-6.69 (m, 20 H, Ph-CH₂-oxazoline and Ph-CH₂-CH₂-CH- in backbone chain), 6.69-6.62 (m, 210 H, O=C-NH-CH in NIPAAm), 4.00-3.68 (m, 215 H, -CH-CH₂- of backbone chain in NIPAAm, -CH-CH₂- of backbone chain in oxazoline and S=C-CH₂-CH₃ in backbone chain), 3.58-3.49 (m, 426 H, -CH-CH₂- of backbone chain in NIPAAm and -O-CH₂-CH-N- in oxazoline), 2.05-1.82 (m, 218 H, CH₃-CH-CH₃ in NIPAAm, Ph-CH₂-oxazoline, -O-CH₂-CH-N- in oxazoline and Ph-CH₂-CH₂-CH- in

backbone chain), 1.73-1.43 (m, 6 H, -CH-CH₂- of backbone chain in oxazoline), 1.33-1.20 (m, 1260 H, CH₃-CH-CH₃ in NIPAAm), 1.19-1.14 (m, 3 H, S=C-CH₂-CH₃ in backbone chain). GPC (THF): *M_n* = 24519, *M_w* = 25499, PDI = 1.04.

Synthesis of Fe^{II}-PN_xO_y (x=120, y=4; x=150, y=3; x=210, y=3): A highly diluted solution of PN_xO_y (x=120, y= 4; x=150, y= 3; x= 210, y= 3) (8.0 mmol) in THF (50 mL) was added dropwise to a stirred solution of FeCl₂ (8.8 mmol, 1.12 g) in THF (20 mL) at 25 °C. The mixtures were stirred at room temperature for 10 h and then were concentrated in vacuo. Crude products were subsequently precipitated in cold *n*-pentane (100 mL). Filtration and drying in vacuum afforded Fe^{II}-PN_xO_y as the brown powder. **Fe^{II}-PN₁₂₀O₄:** FT-IR (KBr): $\gamma_{\text{max}}/\text{cm}^{-1}$ 3533, 3302, 3080, 2973, 2931, 2877, 1727, 1652, 1526, 1457, 1380, 1368, 1334, 1261, 1167, 1031, 971, 917, 881, 840, 702, 671, 609, 509. $\alpha_{\text{D}}^{20} = -32.9$ (C = 0.005 g/mL, THF), iron content: 0.092 mmol/g. Cloud-point of Fe^{II}-PN₁₂₀O₄ was ca. 26 °C. **Fe^{II}-PN₁₅₀O₃:** FT-IR (KBr): $\gamma_{\text{max}}/\text{cm}^{-1}$ 3533, 3300, 3082, 2975, 2934, 2878, 1725, 1652, 1524, 1455, 1377, 1367, 1335, 1261, 1172, 1031, 970, 916, 885, 841, 702, 673, 606, 507. $\alpha_{\text{D}}^{20} = -29.6$ (C = 0.005 g/mL, THF), iron content: 0.069 mmol/g. Cloud-point of Fe^{II}-PN₁₅₀O₃ was ca. 29 °C. **Fe^{II}-PN₂₁₀O₃:** FT-IR (KBr): $\gamma_{\text{max}}/\text{cm}^{-1}$ 3533, 3302, 3083, 2974, 2937, 2875, 1729, 1652, 1527, 1456, 1381, 1368, 1335, 1261, 1172, 1030, 972, 919, 880, 843, 702, 673, 610, 509. $\alpha_{\text{D}}^{20} = -37.8$ (C = 0.005 g/mL, THF), iron content: 0.042 mmol/g. Cloud-point of Fe^{II}-PN₂₁₀O₃ was ca. 31 °C.

Preparation of Neat-C

To evaluate the importance of polymeric pockets around active sites, Neat-C was prepared as the control catalyst. 4-benzyl-2-vinylloxazoline (5.0 mmol, 0.94 g) was dissolved in THF (20 mL). FeCl₂ (5.5 mmol, 0.70 g) in THF (50 mL) was added dropwise into the above solution under vigorous stirring. The mixture was stirred at room temperature for 10 h, and then concentrated in vacuum. Product was precipitated in cold *n*-pentane (100 mL). Filtration and drying in vacuum afforded the Neat-C as a brown powder. FT-IR (KBr): $\gamma_{\text{max}}/\text{cm}^{-1}$ 3264, 3150, 2946, 1959, 1916, 1726, 1652, 1574, 1494, 1447, 1402, 1158, 1033, 1007, 856, 815, 746, 702, 687, 572, 493. $\alpha_{\text{D}}^{20} = -33.4$ (C = 0.005 g/mL, THF), iron content: 1.41 mmol/g.

Job's plot to determine the stoichiometry of Fe(II) ion in Fe^{II}-PN_xO_y

Stoichiometry of Fe(II) ion in Fe^{II}-PN_xO_y was determined by Job's method. A series of solutions (3 mL) containing PN_xO_y (x=120, y= 4; x=150, y= 3; x= 210, y= 3) and FeCl₂ with different molar ratio were prepared in THF. The sum of the total concentration of oxazoline in PN_xO_y and Fe(II) ion remained constant (0.01 mol.L⁻¹). Molar fraction of Fe(II) ion was varied from 0.1 to 1.0. The absorbance at 297 nm where the Fe^{II}-oxazoline complex shows a maximum absorbance was measured. The resultant absorbance was corrected to account for the absorbance of free Fe(II) ion. The corrected absorbance was plotted against the mole fraction of iron.

Asymmetric SMA of thiols to α , β -unsaturated ketones in water

Fe^{II}-PN_xO_y (3 mol% of ketones based on iron content) and α , β -unsaturated ketones (0.1 mmol) were stirred in water (1.0 mL) for 5 min. Thiol (0.12 mmol) was then added. The resulting mixture was stirred at 25 °C until the reaction was judged to be complete based on TLC analysis. Then reaction mixture was heated to above 36 °C, and held at this temperature for 5 min to make catalyst completely precipitate from the

aqueous system. The precipitated catalyst was washed with ether (3×5.0 mL), dried at room temperature in vacuum, and finally recharged with fresh substrate for the next catalytic cycle. Supernatant separated from reaction system was extracted with dichloromethane (3×0.5 mL).

5 Combined organic phase was dried with anhydrous Na_2SO_4 and concentrated in vacuum. Further purification of the residue by chromatography on silica gel (Acros, 40–60 μm , 60 \AA , eluent: petroleum ether/ethyl acetate = 5/1 (v/v)) afforded the desired chiral adducts. All products of **1-7** were identified by ^1H NMR spectra. Their enantiomeric
10 excess (ee) values were determined by high performance liquid chromatography (HPLC) analysis using the Daicel Chiralpak AD columns. Detailed NMR spectra and HPLC analysis for the products of **1-7** were available in the ESI.†

(*S*)-3-(Propylthio)-1,3-diphenylpropan-1-one (**1**): Yield: 95%,
15 determined by isolated yield after column chromatography. Ee value: 96%, determined by HPLC (iPrOH/n-hexane = 10:90 (v/v)), flow rate = $1.0 \text{ mL} \cdot \text{min}^{-1}$, 25°C , $\lambda = 254 \text{ nm}$, major enantiomer $t_{\text{S}} = 5.75 \text{ min}$, minor enantiomer $t_{\text{R}} = 4.82 \text{ min}$. ^1H NMR (CDCl_3 , 500 MHz): δ (ppm): 7.95–7.46 (m, 5 H, *Ph*-CO-CH₂-), 7.45–7.15 (m, 5 H, *Ph*-CH-S-), 4.59–4.56 (m,
20 1 H, CH-CH₂-CO-), 3.57–3.56 (d, 2 H, CH-CH₂-CO-), 2.41–2.23 (m, 2 H, -S-CH₂-CH₂-), 1.60–1.49 (m, 2 H, S-CH₂-CH₂-CH₃), 0.94–0.91 (m, 3 H, S-CH₂-CH₂-CH₃).

(*S*)-4-(Propylthio)-4-phenylbutan-2-one (**2**): Yield: 96%, determined
25 by isolated yield after column chromatography. Ee value: 99%, determined by HPLC (iPrOH/n-hexane = 20:80 (v/v)), flow rate = $1.0 \text{ mL} \cdot \text{min}^{-1}$, 25°C , $\lambda = 254 \text{ nm}$, major enantiomer $t_{\text{S}} = 6.12 \text{ min}$, minor enantiomer $t_{\text{R}} = 4.74 \text{ min}$. ^1H NMR (CDCl_3 , 500 MHz): δ (ppm): 7.55–7.31 (m, 5 H, *Ph*-CH-S-), 4.49–4.46 (m, 1 H, CH-CH₂-CO-), 3.25–3.24 (d,
30 2 H, CH-CH₂-CO-), 2.39–2.23 (m, 2 H, -S-CH₂-CH₂-CH₃), 1.57–1.53 (m, 2 H, -S-CH₂-CH₂-CH₃), 1.36 (s, 3 H, -CO-CH₃), 0.96–0.91 (m, 3 H, -S-CH₂-CH₂-CH₃).

(*S*)-3-(Propylthio)-3-(4-methoxyphenyl)-1-phenylpropan-1-one (**3**):
Yield: 92%, determined by isolated yield after column chromatography. Ee value: 98%, determined by HPLC (iPrOH/n-hexane = 20:80 (v/v)),
35 flow rate = $1.0 \text{ mL} \cdot \text{min}^{-1}$, 25°C , $\lambda = 254 \text{ nm}$, major enantiomer $t_{\text{S}} = 12.32 \text{ min}$; minor enantiomer $t_{\text{R}} = 10.08 \text{ min}$. ^1H NMR (CDCl_3 , 500 MHz): δ (ppm): 7.94–7.43 (m, 5 H, *Ph*-CO-CH₂-), 7.39–6.82 (m, 4 H, CH₃O-*Ph*-CH-), 4.56–4.53 (m, 1 H, CH-CH₂-CO-), 3.81 (s, 3 H, CH₃O-*Ph*-CH-), 3.57–3.48 (d, 2 H, CH-CH₂-CO-), 2.38–2.23 (m, 2 H, -S-CH₂-CH₂-CH₃),
40 1.60–1.49 (m, 2 H, -S-CH₂-CH₂-CH₃), 0.97–0.88 (m, 3 H, -S-CH₂-CH₂-CH₃).

(*S*)-4-(Propylthio)-4-(4-methoxyphenyl) butan-2-one (**4**): Yield: 95%,
determined by isolated yield after column chromatography. Ee value: 90%, determined by HPLC (iPrOH/n-hexane = 10:90 (v/v)), flow rate =
45 $1.0 \text{ mL} \cdot \text{min}^{-1}$, 25°C , $\lambda = 254 \text{ nm}$, major enantiomer $t_{\text{S}} = 11.04 \text{ min}$, minor enantiomer $t_{\text{R}} = 8.11 \text{ min}$. ^1H NMR (CDCl_3 , 500 MHz): δ (ppm): 7.75–6.91 (m, 4 H, CH₃O-*Ph*-CH-), 4.40–4.30 (m, 1 H, CH-CH₂-CO-), 3.92–3.87 (d, 2 H, CH-CH₂-CO-), 2.64 (s, 3 H, CH₃O-*Ph*-CH-), 2.28–2.23 (m, 2 H, -S-CH₂-CH₂-CH₃), 2.09–2.01 (m, 2 H, -S-CH₂-CH₂-CH₃), 1.40 (s, 3 H,
50 -CO-CH₃), 0.92–0.85 (m, 2 H, -S-CH₂-CH₂-CH₃).

(*S*)-3-(Propylthio)-3-(4-nitrophenyl)-1-phenylpropan-1-one (**5**): Yield:
10%, determined by isolated yield after column chromatography. Ee value: 89%, determined by HPLC (iPrOH/n-hexane = 30:70 (v/v)), flow
rate = $1.0 \text{ mL} \cdot \text{min}^{-1}$, 25°C , $\lambda = 254 \text{ nm}$, major enantiomer $t_{\text{S}} = 11.78 \text{ min}$,
55 minor enantiomer $t_{\text{R}} = 10.01 \text{ min}$. ^1H NMR (CDCl_3 , 500 MHz): δ (ppm): 8.20–7.81 (m, 4 H, NO₂-*Ph*-CH-), 7.75–7.46 (m, 5 H, *Ph*-CO-CH₂-), 4.79–4.50 (m, 1 H, CH-CH₂-CO-), 3.78–3.44 (d, 2 H, CH-CH₂-CO-), 2.50–2.18

(m, 2 H, -S-CH₂-CH₂-CH₃), 1.59–1.52 (m, 2 H, -S-CH₂-CH₂-CH₃), 0.95–0.89 (m, 3 H, -S-CH₂-CH₂-CH₃).

60 (*S*)-3-(4-Chlorobenzylthio)-1,3-diphenylpropan-1-one (**6**): Yield: 93%, determined by isolated yield after column chromatography. Ee value: 95%, determined by HPLC (iPrOH/n-hexane = 20:80 (v/v)), flow rate = $1.0 \text{ mL} \cdot \text{min}^{-1}$, 25°C , $\lambda = 254 \text{ nm}$, major enantiomer $t_{\text{S}} = 8.51 \text{ min}$; minor enantiomer $t_{\text{R}} = 6.42 \text{ min}$. ^1H NMR (CDCl_3 , 500 MHz): δ (ppm): 7.89–
65 7.42 (m, 5 H, *Ph*-CO-CH₂-), 7.40–7.35 (m, 4 H, Cl-*Ph*-CH₂-), 7.28–7.14 (m, 5 H, *Ph*-CH-S-), 4.17–4.12 (m, 1 H, -S-CH-*Ph*), 3.59–3.51 (m, 2 H, -S-CH₂-*Ph*), 3.51–3.44 (m, 2 H, CH-CH₂-CO-).

(*S*)-3-(4-Chlorobenzylthio)-3-(4-methoxyphenyl)-1-phenylpropan-1-one
70 (**7**): Yield: 90%, determined by isolated yield after column chromatography. Ee value: 96%, determined by HPLC (iPrOH/n-hexane = 3:97 (v/v)), flow rate = $1.0 \text{ mL} \cdot \text{min}^{-1}$, 25°C , $\lambda = 254 \text{ nm}$, major enantiomer $t_{\text{S}} = 20.15 \text{ min}$, minor enantiomer $t_{\text{R}} = 17.48 \text{ min}$. ^1H NMR (CDCl_3 , 500 MHz): δ (ppm): 7.33–7.17 (m, 13 H, Cl-*Ph*-CH₂-, CH₃O-*Ph*-CH-, and *Ph*-CO-CH₂-), 4.17–4.15 (m, 1 H, CH-CH₂-CO-), 4.14–4.13 (m,
75 2 H, Cl-*Ph*-CH₂-S-), 3.60 (s, 3 H, CH₃O-*Ph*-CH-), 2.99–2.91 (m, 2 H, CH-CH₂-CO-).

(*S*)-4-(4-Chlorobenzylthio)pentan-2-one (**8**): Yield: 94%, determined
by isolated yield after column chromatography. Ee value: >99%, determined by HPLC (iPrOH/n-hexane = 10:90 (v/v)), flow rate = 1.0
80 $\text{mL} \cdot \text{min}^{-1}$, 25°C , $\lambda = 254 \text{ nm}$, major enantiomer $t_{\text{S}} = 6.07 \text{ min}$, minor enantiomer $t_{\text{R}} = 4.99 \text{ min}$. ^1H NMR (CDCl_3 , 500 MHz): δ (ppm): 7.33–7.27 (m, 4 H, Cl-*Ph*-CH₂-), 3.75–3.74 (m, 2 H, Cl-*Ph*-CH₂-), 3.20–3.13 (m, 1 H, -S-CH-CH₃), 2.73–2.64 (m, 2 H, CH-CH₂-CO-), 2.14 (s, 3 H, -CO-CH₃), 1.64–1.52 (m, 3 H, CH₃-CH-
85 CH₂).

(*S*)-3-(4-Chlorophenylthio)-1,3-diphenylpropan-1-one (**9**): Yield: 92%,
determined by isolated yield after column chromatography. Ee value: 98%, determined by HPLC (iPrOH/n-hexane = 20: 80 (v/v)), flow rate =
90 $1.0 \text{ mL} \cdot \text{min}^{-1}$, 25°C , $\lambda = 254 \text{ nm}$, major enantiomer $t_{\text{S}} = 10.34 \text{ min}$, minor enantiomer $t_{\text{R}} = 8.34 \text{ min}$. ^1H NMR (CDCl_3 , 500 MHz): δ (ppm): 7.44–7.41 (m, 5 H, *Ph*-CO-CH₂-), 7.32–7.29 (m, 9 H, *Ph*-CH-S- and Cl-*Ph*-S-), 2.05–2.03 (m, 1 H, CH-CH₂-CO-), 1.60–1.58 (d, 2 H, CH-CH₂-CO-).

Acknowledgements

The authors are grateful for the financial support provided by
95 the National Natural Science Foundation of China (21676078, 21476069), the Natural Science Foundation of Hunan Province for Distinguished Young Scholar (2016JJ1013), Scientific Research Fund of Hunan Provincial Education Department (19A323), and Science and Technology Planning Project of
100 Hunan Province (2018TP1017). We also thank Dr. Mingjie Zhang, Wenqin Fu, and Ziqiang Xiao for their helpful discussions.

Notes and references

- [1] a) D. Enders, K. Lüttgen and A. A. Narine, *Synthesis*, 2007, **7**, 959; b) X. Wang, Q. Hua, Y. Cheng, Q. Yang, J. Chen and W. Xiao, *Angew. Chem. Int. Ed.*, 2010, **49**, 8379; c) M. N. Grayson and K. N. Houk, *J. Am. Chem. Soc.*, 2016, **138**, 9041; d) Y. Li, S. Zhu and Q. Zhou, *Org. Lett.*, 2019, **21**, 9391.
- [2] a) N. K. Rana, S. Selvakumar and V. K. Singh, *J. Org. Chem.*, 2010, **75**, 2089; b) L. Dai, S. Wang and F. Chen, *Adv. Synth. Catal.*, 2010, **352**, 2137; c) J. Guo and M. W. Wong, *J. Org. Chem.*, 2017, **82**, 4362.
- [3] E. Emori, T. Arai, H. Sasai and M. Shibasaki, *J. Am. Chem. Soc.*, 1998, **120**, 4043.

- [4] a) P. Ricci, A. Carlone, G. Bartoli, M. Bosco, L. Sambri and P. Melchiorre, *Adv. Synth. Catal.*, 2008, **350**, 49; b) N. Fu, L. Zhang, S. Luo and J. Cheng, *Org. Lett.*, 2014, **16**, 4626; c) J. Chen, S. Meng, L. Wang, H. Tang and Y. Huang, *Chem. Sci.*, 2015, **6**, 4184; d) J. Yang, A. J. M. Farley and D. J. Dixon, *Chem. Sci.*, 2017, **8**, 606; e) J. L. Fulton, M. A. Horwitz, E. L. Bruske and J. S. Johnson, *J. Org. Chem.*, 2018, **83**, 3385.
- [5] a) J. D. White and S. Shaw, *Chem. Sci.*, 2014, **5**, 2200; b) S. Shaw and J. D. White, *Org. Lett.*, 2015, **17**, 4564.
- [6] a) P. Gao, A. Li, H. H. Lee, D. I. C. Wang and Z. Li, *ACS Catal.*, 2014, **4**, 3763; b) K. Liu, M. Abass, Q. Zou and X. Yan, *Green Energy Environ.*, 2017, **2**, 58; c) A. Y. Chen, R. N. Adamek, B. L. Dick, C. V. Credille, C. N. Morrison and S. M. Cohen, *Chem. Rev.*, 2019, **119**, 1323.
- [7] a) Q. Luo, C. Hou, Y. Bai, R. Wang and J. Liu, *Chem. Rev.*, 2016, **116**, 13571; b) P. Dydio, H. M. Key, A. Nazarenko, J. Y. E. Rha, V. Seyedkazemi, D. S. Clark and J. F. Hartwig, *Science*, 2016, **354**, 102; c) J. Chen, J. Wang, Y. Bai, K. Li, E. S. Garcia, A. L. Ferguson and S. C. Zimmerman, *J. Am. Chem. Soc.*, 2018, **140**, 13695.
- [8] a) T. Terashima, T. Mes, T. F. A. D. Greef, M. A. J. Gillissen, P. Besenius, A. R. A. Palmans and E. W. Meijer, *J. Am. Chem. Soc.*, 2011, **133**, 4742; b) A. Sanchez-Sanchez, A. Arbe, J. Kohlbrecher, J. Colmenero and J. A. Pomposo, *Macromol. Rapid Commun.*, 2015, **36**, 1592; c) S. Thanneeru, S. S. Duay, L. Jin, Y. Fu, A. M. Angeles-Boza and J. He, *ACS Macro Lett.*, 2017, **6**, 652; d) H. Rothfuss, N. D. Knöfel, P. W. Roesky and C. Barner-Kowollik, *J. Am. Chem. Soc.*, 2018, **140**, 5875.
- [9] a) R. Kikkeri, H. Traboulsi, N. Humbert, E. Gumienna-Kontecka, R. Arad-Yellin, G. Melman, M. Elhabiri, A. M. Albrecht-Gary and A. Shanzler, *Inorg. Chem.*, 2007, **46**, 2485; b) G. C. Hargaden and P. J. Guiry, *Chem. Rev.*, 2009, **109**, 2505.
- [10] P. J. M. Stals, C. Cheng, L. van Beek, A. C. Wauters, A. R. A. Palmans, S. Han and E. W. Meijer, *Chem. Sci.*, 2016, **7**, 2011.
- [11] a) T. Sun and G. Qing, *Adv. Mater.*, 2011, **23**, 57; b) J. Potier, S. Menuel, J. Lyskawa, D. Fournier, F. Stoffelbach, E. Monflier, P. Woisel and F. Hapiot, *Chem. Commun.*, 2015, **51**, 2328; c) S. Kim and H. Choi, *ACS Sustainable Chem. Eng.*, 2019, **7**, 19870.
- [12] a) H. Kakwere and S. Perrier, *J. Am. Chem. Soc.*, 2009, **131**, 1889; b) G. Moad, *Polym. Chem.*, 2017, **8**, 177.
- [13] J. Willenbacher, O. Altintas, P. W. Roesky and C. Barner-Kowollik, *Macromol. Rapid Commun.*, 2014, **35**, 45.
- [14] P. Rawat, R. N. Singh, V. Baboo, P. Niranjana, H. Rani, R. Saxena and S. Ahmad, *J. Mol. Struct.*, 2017, **1129**, 37.
- [15] M. A. Cortez and S. M. Grayson, *Macromolecules*, 2010, **43**, 4081.
- [16] K. N. T. Tseng, J. W. Kampf and N. K. Szymczak, *ACS Catal.*, 2015, **5**, 411.
- [17] (a) M. Zhang, L. Wei, H. Chen, Z. Du, B. P. Binks and H. Yang, *J. Am. Chem. Soc.*, 2016, **138**, 10173; (b) Y. Zhang, R. Tan, M. Gao, P. Hao and D. Yin, *Green Chem.*, 2017, **19**, 1182.
- [18] a) E. J. Olson and P. Bühlmann, *J. Org. Chem.*, 2011, **76**, 8406; b) E. S. Cueny and C. R. Landis, *Organometallics*, 2019, **38**, 926.
- [19] S. K. Garg, R. Kumar and A. K. Chakraborti, *Synlett*, 2005, **9**, 1370.
- [20] B. J. Coe and S. J. Glenwright, *Coord. Chem. Rev.*, 2000, **203**, 5.
- [21] a) A. M. Hanlon, C. K. Lyon, E. B. Berda, *Macromolecules*, 2016, **49**, 2; b) S. Mavila, O. Eivgi, I. Berkovich and N. G. Lemcoff, *Chem. Rev.*, 2016, **116**, 878.
- [22] a) J. A. Pomposo, I. Perez-Baena, F. L. Verso, A. J. Moreno, A. Arbe and J. Colmenero, *ACS Macro Lett.*, 2014, **3**, 767; b) J. Rubio-Cervilla, E. González and J. A. Pomposo, *Nanomaterials*, 2017, **7**, 341.
- [23] M. Li, S. Qi, Y. Jin, W. Yao, S. Zhang and J. Zhao, *J. Colloids Surf., B*, 2014, **123**, 852.
- [24] a) P. Cotanda, A. Lu, J. P. Patterson, N. Petzetakis and R. K. O'Reilly, *Macromolecules*, 2012, **45**, 2377; b) M. Artar, E. R. J. Souren, T. Terashima, E. W. Meijer and A. R. A. Palmans, *ACS Macro Lett.*, 2015, **4**, 1099.
- [25] D. A. Evans, D. Seidel, M. Rueping, H. W. Lam, J. T. Shaw and C. W. Downey, *J. Am. Chem. Soc.*, 2003, **125**, 12692.
- [26] T. W. Greene and P. G. M. Wuts, *J. Am. Chem. Soc.*, 2011, **133**, 17934.
- [27] P. Suresh and K. Pitchumani, *Tetrahedron: Asymmetry*, 2008, **19**, 2037.
- [28] S. Bonollo, D. Lanari, F. Pizzo and L. Vaccaro, *Org. Lett.*, 2011, **13**, 2150.
- [29] S. L. Scott, *ACS Catal.*, 2018, **8**, 8597.

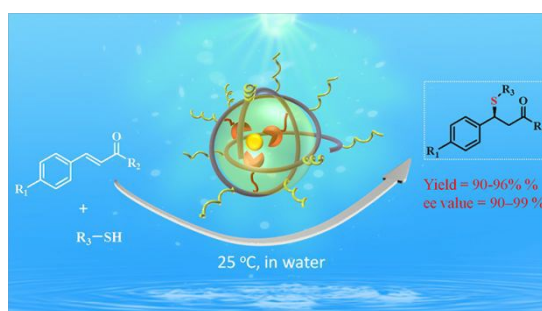
Graphical Abstract

Iron(II)-folded single-chain nanoparticle: a metalloenzyme mimicking sustainable catalyst for highly enantioselective sulfa-Michael addition in water

Weiying Wang, Jiajun Wang, Yibing Pi, Chaoping Li, Rong Tan* and Donghong Yin

National & Local Joint Engineering Laboratory for New Petro-chemical Materials and Fine Utilization of Resources; Key Laboratory of Chemical Biology and Traditional Chinese Medicine Research (Ministry of Education); Key Laboratory of the Assembly and Application of Organic Functional Molecules of Hunan Province, Hunan Normal University, No.36, South Lushan Road, Changsha, Hunan 410081 (P. R. China)

Bio-inspired Fe^{II}-folded SCPNs enabled asymmetric sulfa-Michael addition to be performed in a green and efficient manner, using water as solvent.



* Corresponding authors. Fax: +86-731-8872531. Tel: +86-731-8872576

E-mail: yiyangtanrong@126.com